Supporting Information

Humphry et al. 10.1073/pnas.1003619107

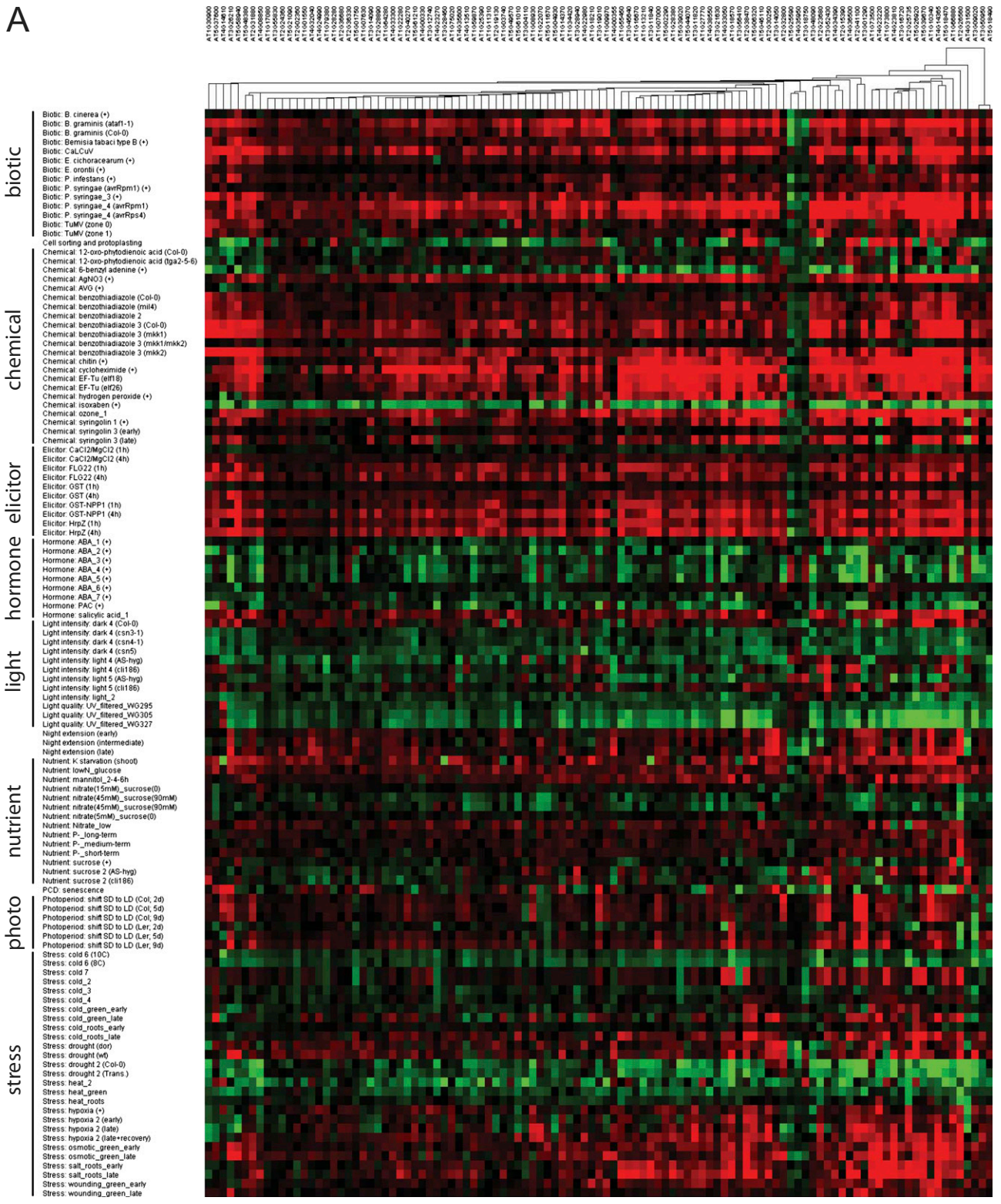

Fig. S1. (Continued)

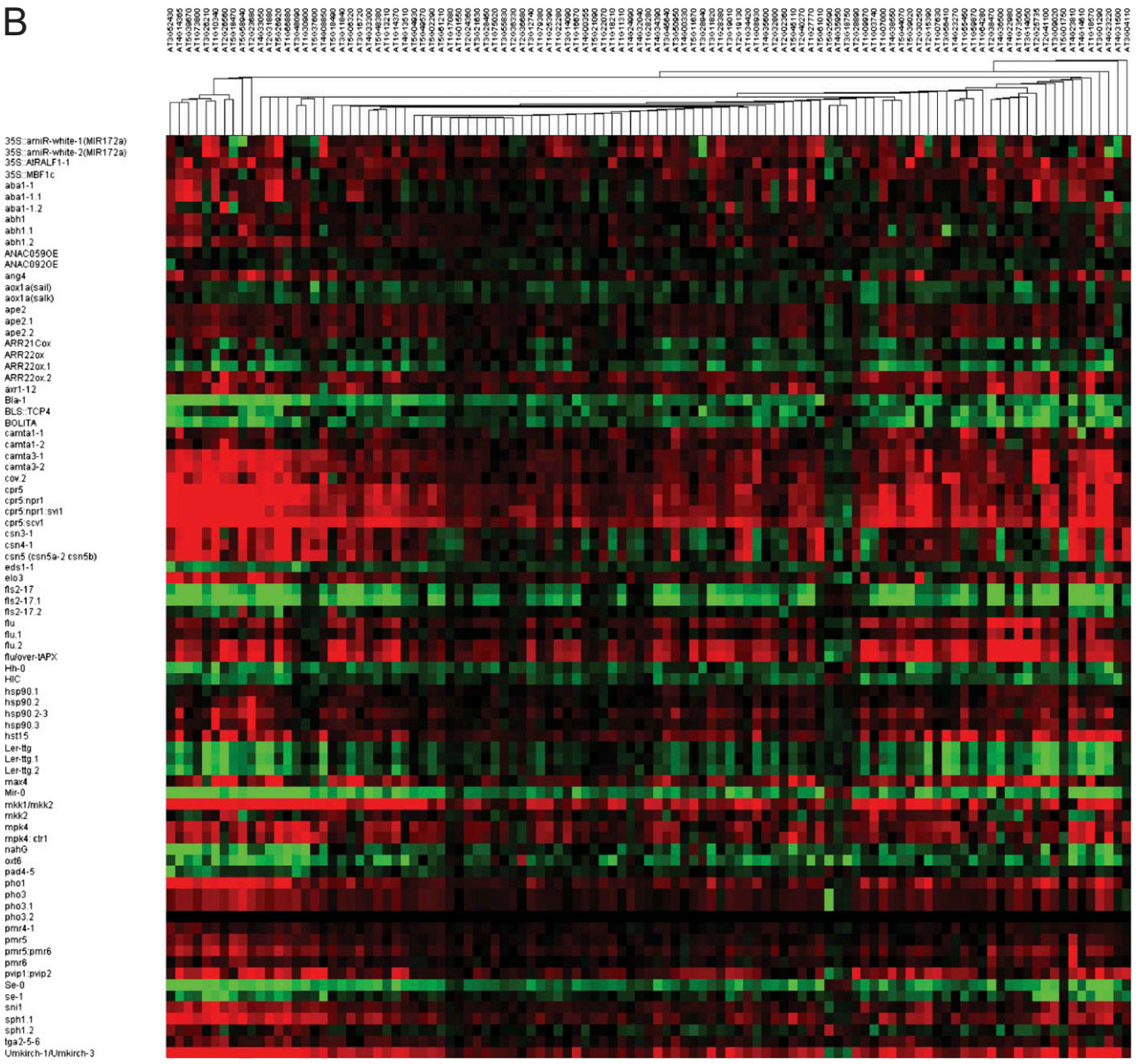

Fig. S1. (Continued)

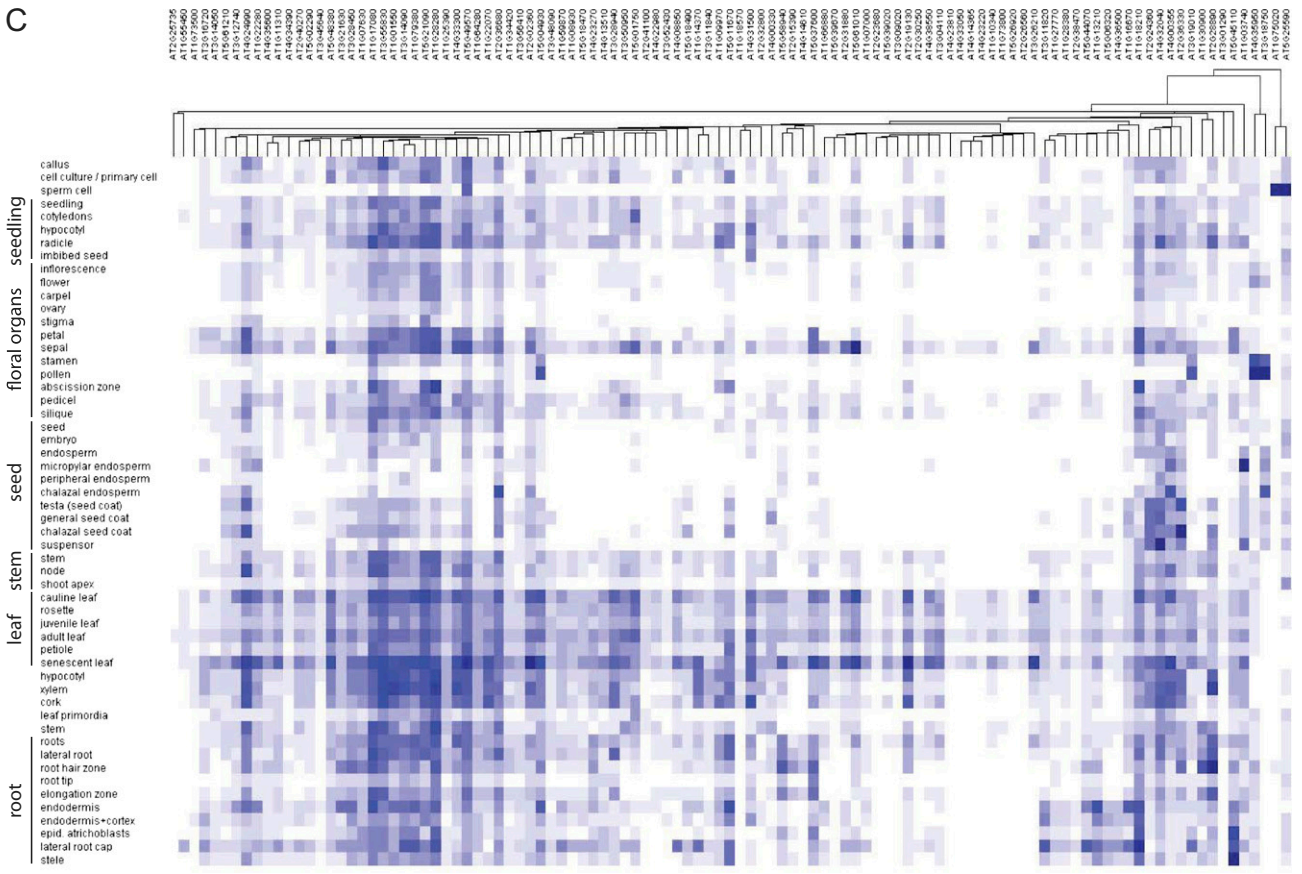

Fig. S1. In silico meta analysis of unique coexpressed genes. Expression analysis of genes found to be coexpressed with *MLO2*, *PEN1*, and *SNAP33* was carried out by using the Web-based tool Genevestigator V3 on the basis of (*A*) stimuli, (*B*) mutations, and (*C*) plant anatomy. For *A* and *B*, relative gene expression is indicated as red or green for up- or down-regulated gene expression, respectively, compared with the relevant control. For *C*, absolute gene expression values (scaled to the expression potential of each gene) are shown, with the darkest for *A* and *B*, respectively, and relative gene expression is indicated by increased darkness of blue color representing the maximum level of expression for a given gene across all measurements (*C*). Data presented in *A* and *B* was trimmed to contain only those conditions that exhibited observable expression changes for the majority of genes examined. Genes were grouped according to their global patterns for each condition via hierarchical clustering.

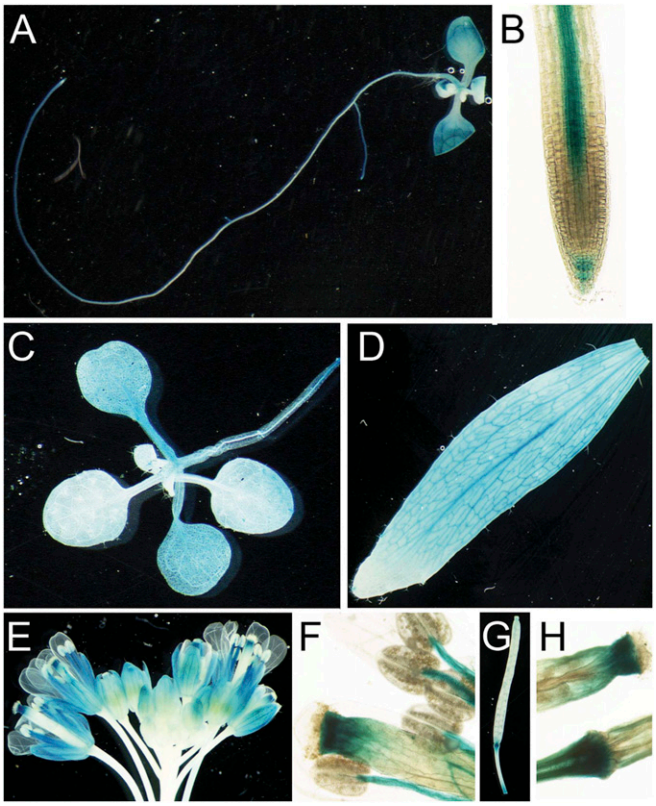

Fig. S2. A unique *cis* element in Arabidopsis controls gene expression in young seedlings and floral organs. Histochemical analysis of different tissues of transgenic Arabidopsis plants expressing a promoter-*GUS* construct containing a tandem repeat of the unique *cis* element (see text). (*A*) Ten-day-old plate-grown seedlings. (*B*) Close-up of roots shown in *A*. (*C*) Two-week-old soil-grown seedlings. (*D*) Cauline leaf. (*E*) Flowers. (*F*) Close-up of floral organs shown in *E*. (*G*) Siliques. (*H*) Close-up of tip (upper) and abscission zone (lower) of siliques shown in (*G*). Similar expression patterns were observed in four independent transgenic lines.

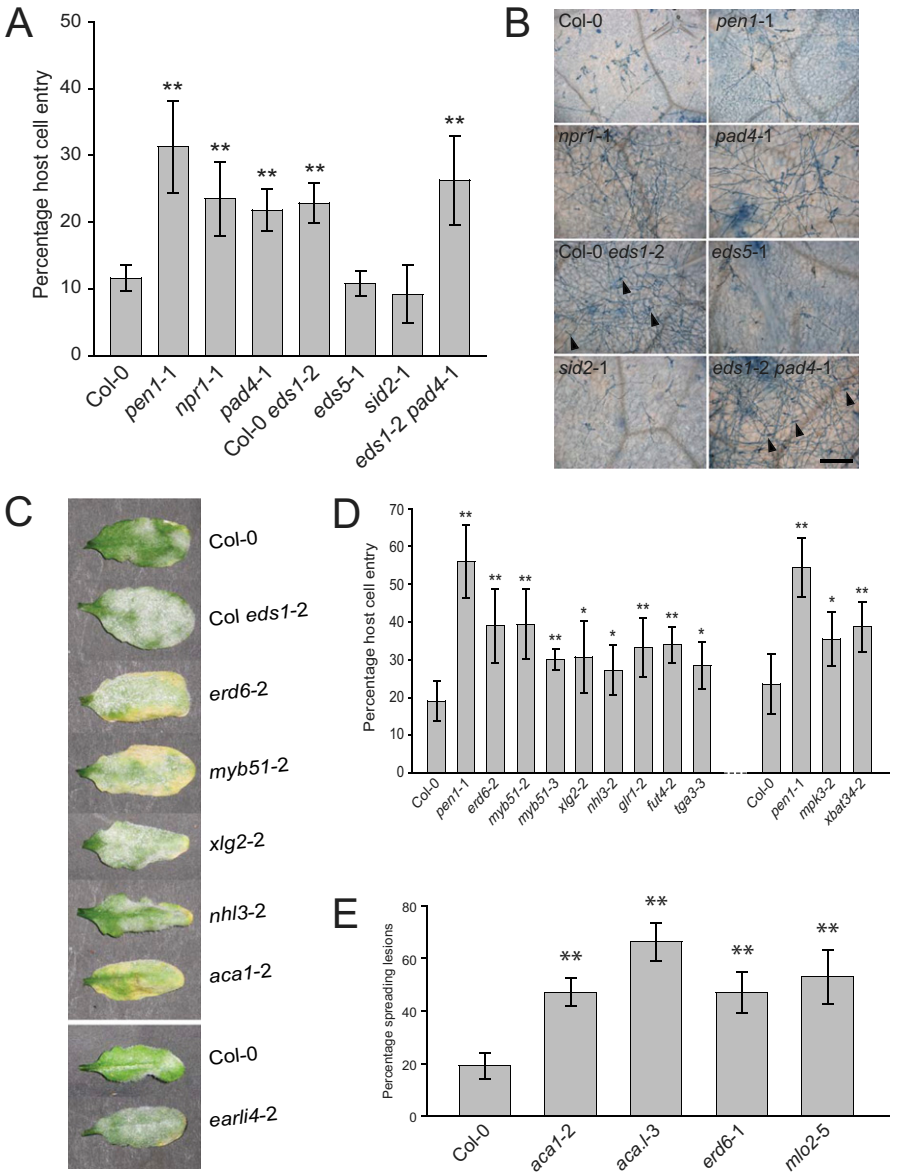

Fig. S3. Mutations in coexpressed genes allow enhanced growth of a range of pathogens with differing lifestyles. (*A*) Quantitative analysis of host cell entry of *E. pisi* on mutants defective in salicylic acid (SA)-based signaling and defense assayed at 3 d after inoculation. Data shown indicate the mean ± SD based on at least five independent leaves. (*B*) Microscopic evaluation of epiphytic *E. pisi* fungal growth (hyphae) on above mutants at 7 d after inoculation. Arrowheads point to asexual reproductive structures (conidiophores). (Scale bar: 100 μm.) (*C*) Representative macroscopic phenotypes of Col-0 and selected insertion lines (second alleles of those shown in Fig. 2) at 10 d after inoculation with *G. orontii*. (*D*) Quantitative analysis of host cell entry of *E. pisi* on second alleles of selected insertion lines shown in Fig. 2 determined at 3 d after inoculation. Results represent mean ± SD of at least five leaves per genotype. (*E*) Quantification of disease symptoms on second alleles of selected insertion lines shown in Fig. 2 6 d after inoculation with *B. cinerea* (*Materials and Methods*). Results represent mean ± SD of three independent samples per genotype. For all data, asterisks indicate a significant difference from Col-0 (*$P \leq 0.05$; **$P \leq 0.01$; Student's *t* test). Comparable results were obtained in at least three (*A*–*D*) or two (*E*) independent experiments.

Dataset S1. List of genes coexpressed with known basal defense components

Dataset S1

Dataset S2. Enriched processes identified in coexpressed genes in Arabidopsis and barley

Dataset S2

Dataset S3. **Coexpressed barley genes (Affymetrix Barley1 contigs) and their HarvEST unigene counterparts**

Dataset S3

Dataset S4. **Coexpressed barley genes (HarvEST unigenes) and their Arabidopsis counterparts**

Dataset S4

Dataset S5. **Overrepresented 6-mer *cis*-acting elements in 5′ upstream regions of coexpressed genes**

Dataset S5

Dataset S6. **Insertional and EMS mutant lines used in this study and their phenotypes**

Dataset S6

Dataset S7. **Microarray experiments used for coexpression analysis**

Dataset S7